Communication

Chelating Ligand Alters the Microscopic Mechanism of Mineral Dissolution

Perry, Owen W. Duckworth, Treavor A. Kendall, Scot T. Martin, and Ralph Mitchell

J. Am. Chem. Soc., **2005**, 127 (16), 5744-5745• DOI: 10.1021/ja042737k • Publication Date (Web): 30 March 2005

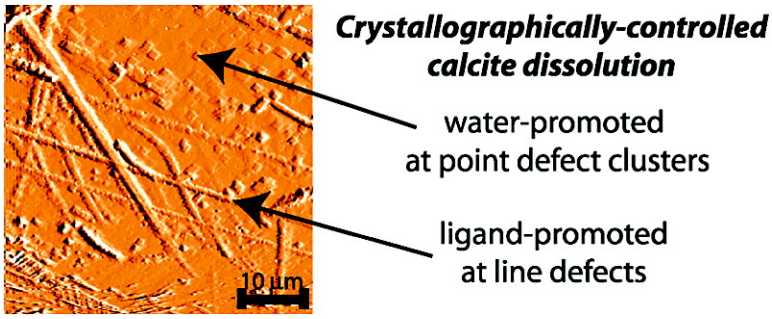

More About This Article

Additional resources and features associated with this article are available within the HTML version:

- Supporting Information
- Links to the 1 articles that cite this article, as of the time of this article download
- Access to high resolution figures
- Links to articles and content related to this article
- Copyright permission to reproduce figures and/or text from this article

View the Full Text HTML

J|A|C|S
COMMUNICATIONS

Published on Web 03/30/2005

Chelating Ligand Alters the Microscopic Mechanism of Mineral Dissolution

Thomas D. Perry, IV, Owen W. Duckworth,† Treavor A. Kendall, Scot T. Martin,* and Ralph Mitchell

Harvard University, Division of Engineering and Applied Sciences, Pierce Hall, Cambridge, Massachusetts 02138

Received December 2, 2004; E-mail: smartin@deas.harvard.edu

The dissolution of calcium carbonate is important in Precambrian and present biology, in the environment, and in industry.[1] Chelating agents can increase calcite dissolution rates[2] through ligand-promoted dissolution.[3,4] As a result, ethylenediamine tetraacetate (EDTA) and other chelators are employed to assist in the dissolution of calcium-bearing minerals for industrial applications, such as the renewal of petroleum wells clogged by calcite[5] and the removal of scale from boilers and heater tubes.[6] Biogenic ligands[7] are also important in regulating calcite dissolution in marine and terrestrial systems.[8]

Surprisingly, the work reported herein shows that EDTA-mediated calcite dissolution occurs via a different process than water-promoted dissolution. The parallel processes of water-dominated dissolution at point defects and ligand-dominated dissolution at linear defects (such as screw defects, line dislocations, dislocation loops, and grain boundaries) are clearly observable in real-time atomic force micrographs. Multiple propagating step edges of differing velocities result. Furthermore, observations in EDTA solutions demonstrate that, after penetration through a critical pit depth barrier, step velocity increases linearly with pit depth for EDTA-promoted dissolution, whereas step velocity in simple water solutions is independent of pit depth.

The calcite ($10\bar{1}4$) surface dissolves by rhombohedral pit formation and subsequent step retreat along the [$\bar{4}41$] and [$48\bar{1}$] crystallographic vectors.[9] The obtuse (*o*) and acute (*a*) pit edges along these vectors have carbonate species that, at the atomic scale, project from or lie in-plane, respectively, with the step edge. These configurations affect relative step velocities (ν_o and ν_a) and thus pit anisotropy during dissolution. (The step edges as described in this communication actually consist of multiple monolayer steps.) The foregoing description has been developed for calcite dissolution in dilute solutions of strong acids or bases.[10] In comparison, the microscopic mechanisms of ligand-promoted calcite dissolution are virtually unexplored.

We measured the macroscopic dissolution rates of calcite in 1−10 mM EDTA and $4 < \text{pH} < 12$ (flow = 1.5 mL min^{-1}).[4,9] The rates increased by as much as 1 order of magnitude (data not shown) over rates measured in the absence of EDTA, a result which is consistent with previous literature reports.[5,11] Concurrent with the macroscopic studies, atomic force microscopy (AFM) showed the evolution of dissolution pits on the surface.

Across a range of pH values and EDTA concentrations, the AFM observations consistently showed two types of pits. Dissolution pits in 3.42 mM EDTA solutions at $4 < \text{pH} < 11$ had a bimodal distribution of pit depths (shallow pits, $z_1 = 17.3 \pm 2.1$ nm, number of pits measured (n) = 41; deep pits, $z_2 = 190 \pm 99$ nm, $n = 16$). An example of a time series of micrographs is shown in Figure 1 for a calcite surface exposed to 3.42 mM EDTA at pH 11.0. Early images in the time series showed a surface with shallow pits ($z <$ 21 nm). Their average step velocity was 1.5 ± 0.1 nm s^{-1},[9] which is consistent with step velocities for water-promoted calcite dissolution (0.7−2.7 nm s^{-1}).[4,10,12,13,14] A second type of pit was also apparent in the time series, namely the progression of a large dissolution pit edge ($z > 120$ nm) oriented along the [$\bar{4}41$] crystallographic vector. The step velocity of the large multilayer step was 10.9 ± 0.6 nm s^{-1}. A relatively pristine terrace region emerged behind the sweeping edge of the pit. The last images in the time series showed that shallow dissolution pits similar to those in the early micrographs (average step velocity of 1.0 ± 0.4 nm s^{-1}) again formed on the renewed terrace.

Step velocity in the presence of EDTA increased as pits deepened as long as the pits surpassed a critical depth value of 25 nm (Figure 1). In 3.42 mM EDTA solutions, the relationship between step

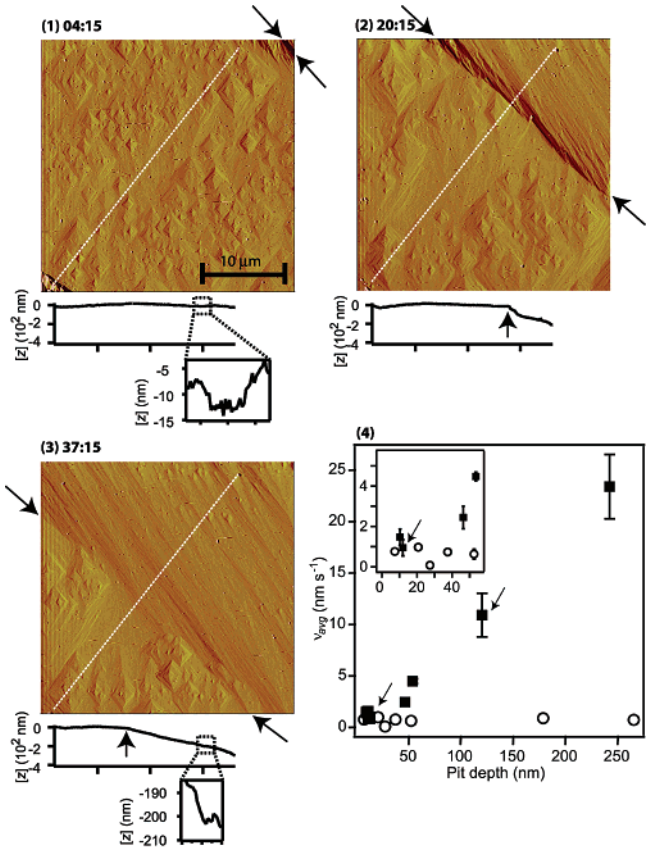

Figure 1. Panels 1−3 show an example of a time series of deflection-mode images captured in the same scan direction of the ($10\bar{1}4$) calcite surface in 3.42 mM EDTA at pH 11.0 showing simultaneous occurrence of shallow and deep dissolution pits. Cross-section profiles, indicated by white dashed lines, are taken from height-mode data. Sample tilt is corrected in the cross sections by subtracting the slope of the terrace preceding the large dissolution wave. Panel 4 summarizes experiments on the dependence of step velocity on pit depth in water (○) and in 3.42 mM EDTA (■) solutions for $5.8 < \text{pH} < 10.9$ on the ($10\bar{1}4$) calcite surface. Uncertainties are estimated from the standard deviation of the velocities of several pits within a time series.

† Present Address: University of California, Department of Civil and Environmental Engineering, Berkeley, California 94720.

10.1021/ja042737k CCC: $30.25

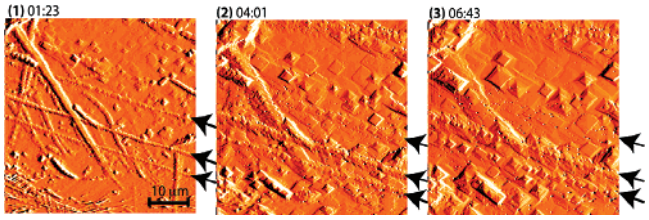

Figure 2. Time series of deflection-mode images (50 μm × 50 μm) of the (10$\bar{1}$4) calcite surface in 3.42 mM EDTA at pH 9.24. EDTA-directed dissolution at linear defects, which allows penetration through a critical depth of 25 nm, results in an increased step velocity. Pits associated with observable linear defects are apparent (see arrows). Image 1 corresponds to a freshly cleaved surface. The surface becomes heavily pitted along the linear defects in images 2 and 3.

velocity (v_{avg}) and pit depth (z) was $v_{avg} = 0.1\ z - 1.4$ for $25 < z < 250$ nm, and there was no dependence on pH over the range investigated. In contrast, the step velocity of shallow pits was independent of pit depth in this study, in agreement with observations of water-promoted dissolution.[4,10,12,13,14] The critical pit depth for increased step velocity in EDTA solutions is apparent in the inset. Simultaneous observation of slow and fast step velocities in EDTA solutions is possible, as highlighted by arrows that indicate data collected from the same sample surface.

The increase of step velocity in EDTA solutions is rationalized by attributing the shallow, slower pits to clusters of point defects[15] dominantly attacked by water and the deeper, faster pits to linear defects dominantly attacked by EDTA. Small, shallow, flat-bottomed, randomly dispersed pits occur on terraces, an observation which is consistent with initiation by water attack at randomly dispersed clusters of point defects.[9,14,16] Dissolution pits initiated at clusters of point defects do not develop into deep pits (i.e., greater than 25 nm), and therefore, the step velocity does not increase in the presence of EDTA. In contrast, linear defects, such as dislocations or grain boundaries that extend deeply into the mineral lattice, result in deep pits (>25 nm) in carbonate minerals.[9,14] The time series of images in Figure 2 shows that dissolution pits with fast step velocities and deep mineral penetration are associated with linear defects.

Pit morphology also indicated differences between water- and EDTA-promoted dissolution. Shallow pits (<25 nm) remained less anisotropic in both neat (average $v_o/v_a = 1.19 \pm 0.18$, $n = 6$) and EDTA (average $v_o/v_a = 1.25 \pm 0.14$, $n = 7$) solutions. In contrast, deep pits in EDTA solutions were more anisotropic (average $v_o/v_a = 2.71 \pm 0.33$, $n = 2$) in this study, in agreement with earlier experiments in EDTA[11] and biogenic-ligand[4] solutions. The differences in pit shape provided further evidence that water-promoted dissolution dominated at shallow pits initiated at clusters of point defects and EDTA-promoted dissolution dominated at deep pits initiated at linear defects.

The preferential attack of EDTA along deeply penetrating crystallographic defects may have been related to facilitated chelation of calcium by EDTA[4] because of increased cation reactivity, increased step density and reaction area, or altered atomic geometry along these lattice features.[17] A further possibility is that, in the absence of EDTA, dissolving species such as aqueous calcium may accumulate near the numerous, highly reactive steps that are characteristic of a deeply penetrating feature, thus resulting in a decrease in localized aqueous undersaturation near the retreating steps and therefore a decrease in step velocity.[13,18] However, with EDTA present to chelate the dissolving calcium and therefore increase undersaturation, rapid step retreat can continue.

The EDTA-promoted dissolution of deep pits, at step velocities up to 20-fold faster than those of water-driven pits, altered step wave velocities and thereby increased the global surface retreat rate and the macroscopic dissolution rate.[19] The discovery of a link between crystallographic features and the chemical mechanism of dissolution (water- versus ligand-) and, consequently, of multiple, simultaneous step velocities highlights the need for further refinement of microscale mechanisms of mineral dissolution.

Acknowledgment. We thank an anonymous reviewer for the insightful suggestion of an alternate mechanism of the effect of EDTA on dissolution. This work was supported in part by Sandia National Laboratories Campus Executive Fellowships, to T.D.P. and O.W.D., the New York Community Trust Merck Fund, the U.S. Department of Energy, the National Science Foundation, and the W. R. Grace Corporation.

Supporting Information Available: Animated time series of deflection-mode images of calcite dissolution in an EDTA solution. This material is available free of charge via the Internet at http://pubs.acs.org.

References

(1) (a) Brown, G. E. *Science* **2001**, *294*, 67−70. (b) Rinck-Pfeiffer, S.; Ragusa, S.; Sztajnbok, P.; Vandevelde, T. *Water Res.* **2000**, *34*, 2110−2118. (c) Schlesinger, W. H. *Biogeochemistry: An Analysis of Global Change*; Academic Press: San Diego, 1997.
(2) Newman, D. K.; Banfield, J. F. *Science* **2002**, *296*, 1071−1077.
(3) Ludwig, C.; Casey, W. H.; Rock, P. A. *Nature* **1995**, *375*, 44−47.
(4) Perry, T. D., IV; Duckworth, O. W.; McNamara, C. J.; Martin, S. T.; Mitchell, R. *Environ. Sci. Technol.* **2004**, *38*, 3040−3046.
(5) Fredd, C. N.; Fogler, H. S. *J. Colloid Interface Sci.* **1998**, *204*, 187−194.
(6) (a) Moore, R. E.; Brennema, D. R.; Bischof, A. E.; Robins, J. D. *Mater. Prot. Perform.* **1972**, *11*, 41. (b) Jamialahmadi, M.; Mullersteinhagen, H. *Heat Transfer Eng.* **1991**, *12*, 19−26.
(7) (a) Orme, C. A.; Noy, A.; Wierzbicki, A.; McBride, M.; Grantham, M.; Teng, H. H.; Dove, P. M.; De Yoreo, J. J. *Nature* **2001**, *411*, 775−779. (b) Teng, H. H.; Dove, P. M.; Orme, C. A.; De Yoreo, J. J. *Science* **1998**, *282*, 724−727.
(8) (a) Pilson, M. *An Introduction to the Chemistry of the Sea*. Prentice Hall: Upper Saddle River, NJ, 1998. (b) Stumm, W.; Morgan, J. J. *Aquatic Chemistry* Wiley: New York, 1996.
(9) Duckworth, O. W.; Martin, S. T. *Am. Mineral.* **2004**, *89*, 554−563.
(10) Arvidson, R. S.; Ertan, I. E.; Amonette, J. E.; Luttge, A. *Geochim. Cosmochim. Acta* **2003**, *67*, 1623−1634.
(11) Friis, A. K.; Davis, T. A.; Figueira, M. M.; Paquette, J.; Mucci, A. *Environ. Sci. Technol.* **2003**, *37*, 2376−2383.
(12) (a) Liang, Y.; Baer, D. R.; McCoy, J. M.; Amonette, J. E.; LaFemina, J. P. *Geochim. Cosmochim. Acta* **1996**, *60*, 4883−4887. (b) Shiraki, R.; Rock, P. A.; Casey, W. H. *Aquat. Geochem.* **2000**, *6*, 87−108. (c) Jordan, G.; Rammensee, W. *Geochim. Cosmochim. Acta* **1998**, *62*, 941−947.
(13) Lea, A. S.; Amonette, J. E.; Baer, D. R.; Liang, Y.; Colton, N. G. *Geochim. Cosmochim. Acta* **2001**, *65*, 369−379.
(14) MacInnis, I. N.; Brantley, S. L. *Geochim. Cosmochim. Acta* **1992**, *56*, 1113−1126.
(15) (a) Macinnis, I. N.; Brantley, S. L. *Chem. Geol.* **1993**, *105*, 31−49. (b) MacInnis, I. N.; Brantley, S. L. *Geochim. Cosmochim. Acta* **1992**, *56*, 1113−1126.
(16) Teng, H. H. *Geochim. Cosmochim. Acta* **2004**, *68*, 253−262.
(17) (a) Barwise, A. J.; Compton, R. G.; Unwin, P. R. *J. Chem. Soc., Faraday Trans.* **1990**, *86*, 137−144. (b) Compton, R. G.; Pritchard, K.; Unwin, P.; Grigg, G.; Silvester, P.; Lees, M.; House, W. *J. Chem. Soc., Faraday Trans.* **1989**, *85*, 4335−4366.
(18) Plummer, L. N.; Packhurst, D. L.; Wigley, T. L. M. *Am. J. Sci.* **1978**, *278*, 179−219.
(19) Lasaga, A.; Luttge, A. *Science* **2001**, *291*, 2400−2404.

JA042737K